

DESY 95-040  
March 1995

## Equivalence of the Parke-Taylor and the Fadin-Kuraev-Lipatov amplitudes in the high-energy limit

Vittorio Del Duca  
Deutsches Elektronen-Synchrotron  
DESY, D-22603 Hamburg , GERMANY

### Abstract

We give a unified description of tree-level multigluon amplitudes in the high-energy limit. We represent the Parke-Taylor amplitudes and the Fadin-Kuraev-Lipatov amplitudes in terms of color configurations that are ordered in rapidity on a two-sided plot. We show that for the helicity configurations they have in common the Parke-Taylor amplitudes and the Fadin-Kuraev-Lipatov amplitudes coincide.

# 1 Introduction

In high-energy hadron collisions multi-jet events are of phenomenological interest because they appear as background to top-quark and electroweak-boson production and to eventual Higgs-boson production and new-physics signals. To compute the production rate for multi-jet events, we need to evaluate amplitudes with multi-parton final states. These are also of interest *per se* because they yield the radiative corrections to the total parton cross section, which in the high-energy limit of perturbative QCD is predicted to have a power-like growth in the parton center-of-mass energy  $\sqrt{\hat{s}}$  [1]-[3].

Multi-parton amplitudes have been computed in the high-energy limit by Fadin, Kuraev and Lipatov (FKL) [2], who considered the tree-level production of  $n$  gluons in parton-parton scattering in the limit of a strong rapidity ordering of the produced partons, assuming their transverse momenta to be all of the same size,  $Q$ . This kinematic configuration is termed *multiregge kinematics*. The amplitudes are given by the exchange of a gluon ladder between the scattering partons (Fig.4). FKL made also an ansatz for the leading logarithmic contribution, in  $\ln(\hat{s}/Q^2)$ , of the loop corrections to the multi-parton amplitudes, to all orders in  $\alpha_s$ . This changes the form of the propagators of the gluons exchanged in the  $\hat{t}$  channel, but preserves the ladder structure of the amplitudes. Using then  $\hat{s}$ -channel unitarity and dispersion relations, FKL computed the total cross section for a one-gluon ladder exchange and the elastic amplitude for the exchange of a two-gluon ladder in a color-singlet configuration, i.e. for the exchange of a perturbative pomeron.

On the other hand, exact tree-level amplitudes for the production of  $n$  gluons have

been computed by Parke and Taylor (PT) [4] in a helicity basis, for specific helicity configurations of the incoming and outgoing gluons. In a helicity basis the color structure of the tree-level amplitudes may be decomposed as a sum over all the noncyclic permutations of the gluon color flows. In a previous work [5] we have represented the color flows of the PT amplitudes in terms of color lines in the fundamental representation of  $SU(N_c)$ . Permuting the color flows the color lines appear twisted, however every configuration may be untwisted introducing a two-sided plot [6]. We have shown then that restricting the PT amplitudes to the multiregge kinematics only the untwisted configurations with the gluons ordered in rapidity on the two-sided plot contribute. In ref.[5] we worked with the squared PT amplitudes at leading  $N_c$ , however due to the incoherence of the leading  $N_c$  term in the color sum of the squared PT amplitudes, the color flows we consider there are the same as the ones of the PT amplitudes themselves. Thus, also for the PT amplitudes, for which no approximation in  $N_c$  is made, the leading color configurations are the ones with the gluons ordered in rapidity on the two-sided plot.

In this paper we consider again the sum over the leading color flows of the PT amplitudes in the multiregge kinematics, and we show that for the helicity configurations they have in common the PT amplitudes and the FKL amplitudes are equal.

Besides, we note that the two helicities of each gluon emitted along the gluon ladder contribute to the same extent to the FKL amplitude, since changing the helicity of a gluon along the ladder changes the FKL amplitude only by a phase.

## 2 Spinor algebra in multiregge kinematics

We consider the production of  $n + 2$  gluons of momentum  $p_i$ , with  $i = 0, \dots, n + 1$  and  $n \geq 0$ , in the scattering between two gluons of momenta  $p_A$  and  $p_B$ , and we assume that the produced gluons satisfy the multiregge kinematics, i.e. we require that the gluons are strongly ordered in rapidity  $y$  and have comparable transverse momentum,

$$y_0 \gg y_1 \gg \dots \gg y_{n+1}; \quad |p_{i\perp}| \simeq |p_{\perp}|. \quad (1)$$

The Mandelstam invariants (38) (Appendix A) take then the approximate form,

$$\begin{aligned} \hat{s} &\simeq |p_{0\perp}| |p_{n+1\perp}| e^{y_0 - y_{n+1}}, \\ \hat{s}_{Ai} &\simeq -|p_{0\perp}| |p_{i\perp}| e^{y_0 - y_i}, \\ \hat{s}_{Bi} &\simeq -|p_{i\perp}| |p_{n+1\perp}| e^{y_i - y_{n+1}}, \\ \hat{s}_{ij} &\simeq |p_{i\perp}| |p_{j\perp}| e^{|y_i - y_j|}. \end{aligned} \quad (2)$$

In the calculation of helicity amplitudes, polarization vectors are expressed in terms of massless spinors. Thus, we recall here and in Appendix B concepts and notations of spinor algebra. Massless Dirac spinors  $\psi_{\pm}(p)$  of fixed helicity are defined by the projection,

$$\psi_{\pm}(p) = \frac{1 \pm \gamma_5}{2} \psi(p). \quad (3)$$

We use for the spinors the shorthand notation of ref.[7],

$$\begin{aligned} \psi_{\pm}(p) &= |p\pm\rangle, \quad \overline{\psi_{\pm}(p)} = \langle p\pm|, \\ \langle pk \rangle &= \langle p - |k+\rangle = \overline{\psi_-(p)} \psi_+(k), \\ [pk] &= \langle p + |k-\rangle = \overline{\psi_+(p)} \psi_-(k). \end{aligned} \quad (4)$$

In the multiregge kinematics the spinor products (46), computed in Appendix B, reduce to

$$\begin{aligned}
\langle p_i p_j \rangle &\simeq -\sqrt{\frac{|p_{i\perp}|}{|p_{j\perp}|}} p_{j\perp} \exp\left(\frac{y_i - y_j}{2}\right) \quad \text{for } y_i > y_j, \\
\langle p_A p_i \rangle &\simeq -\sqrt{\frac{|p_{0\perp}|}{|p_{i\perp}|}} p_{i\perp} \exp\left(\frac{y_0 - y_i}{2}\right), \\
\langle p_i p_B \rangle &\simeq -\sqrt{|p_{i\perp}| |p_{n+1\perp}|} \exp\left(\frac{y_i - y_{n+1}}{2}\right), \\
\langle p_A p_B \rangle &\simeq -\sqrt{|p_{0\perp}| |p_{n+1\perp}|} \exp\left(\frac{y_0 - y_{n+1}}{2}\right),
\end{aligned} \tag{5}$$

where we have used the complex notation (36) and we have expressed  $p_A^+$  and  $p_B^-$  through the momentum conservation (37) (Appendix A) and kept only the leading contribution.

### 3 Parke-Taylor amplitudes in multiregge kinematics

After having set up the kinematics we are going to use in this and in the next section, we introduce the PT amplitudes, i.e. exact tree-level amplitudes for the production of  $n$  gluons in a specific helicity configuration. Sorting out the color structure, a tree-level multigluon amplitude in a helicity basis may be written as [8]

$$M_n = \sum_{[A,0,\dots,n+1,B]} \text{tr}(\lambda^a \lambda^{d_0} \dots \lambda^{d_{n+1}} \lambda^b) m(\tilde{p}_A, \epsilon_A; p_0, \epsilon_0; \dots; p_{n+1}, \epsilon_{n+1}; \tilde{p}_B, \epsilon_B), \tag{6}$$

where  $a, d_0, \dots, d_{n+1}, b$ , and  $\epsilon_A, \epsilon_0, \dots, \epsilon_B$  are respectively the colors and the polarizations of the gluons, the  $\lambda$ 's are the color matrices in the fundamental representation of  $SU(N_c)$  and the sum is over the noncyclic permutations of the set  $[A, 0, \dots, B]$ . The gauge-invariant subamplitudes,  $m(\tilde{p}_A, \epsilon_A; p_0, \epsilon_0; \dots; p_{n+1}, \epsilon_{n+1}; \tilde{p}_B, \epsilon_B)$ , are known for a few specific helicity

configurations [4], [9]. Considering all the momenta as outgoing, the PT amplitudes describe the *maximally helicity-violating* configurations  $(-, -, +, \dots, +)$  [4], [8]<sup>1</sup>,

$$im(-, -, +, \dots, +) = i 2^{2+n/2} g^{n+2} \frac{\langle p_i p_j \rangle^4}{\langle \tilde{p}_A p_0 \rangle \dots \langle p_{n+1} \tilde{p}_B \rangle \langle \tilde{p}_B \tilde{p}_A \rangle}, \quad (7)$$

where  $i$  and  $j$  are the gluons of negative helicity. The configurations  $(+, +, -, \dots, -)$  are then obtained by replacing the  $\langle pk \rangle$  products with  $[kp]$  products. In eq.(7) the following representation for the gluon polarization vector has been used [8],

$$\epsilon_\mu^\pm(p, k) = \pm \frac{\langle p \pm | \gamma_\mu | k \pm \rangle}{\sqrt{2} \langle k \mp | p \pm \rangle}, \quad (8)$$

which enjoys the properties

$$\epsilon_\mu^{\pm*}(p, k) = \epsilon_\mu^\mp(p, k), \quad (9)$$

$$\epsilon_\mu^\pm(p, k) \cdot p = \epsilon_\mu^\pm(p, k) \cdot k = 0, \quad (10)$$

$$\sum_{\nu=\pm} \epsilon_\mu^\nu(p, k) \epsilon_\rho^{\nu*}(p, k) = -g_{\mu\rho} + \frac{p_\mu k_\rho + p_\rho k_\mu}{p \cdot k}, \quad (11)$$

where  $k$  is an arbitrary light-like momentum. The sum (11) is equivalent to use an axial, or physical, gauge.

From the spinor products (5), we see that in the multiregge kinematics the PT amplitudes (7) for which the numerator is the largest are the ones for which the pair of negative-helicity gluons is one of the following,

$$(A, B), \quad (A, n+1), \quad (B, 0), \quad (0, n+1). \quad (12)$$

We focus on the first pair, and fix  $\tilde{p}_A = -p_A$  and  $\tilde{p}_B = -p_B$ . From eq.(7) we have,

$$im(-p_A, -; p_0, +; \dots; p_{n+1}, +; -p_B, -) = i 2^{2+n/2} g^{n+2} \frac{\langle p_A p_B \rangle^4}{\langle p_A p_0 \rangle \dots \langle p_{n+1} p_B \rangle \langle p_B p_A \rangle}, \quad (13)$$

---

<sup>1</sup>Note that eq.(7) differs for the  $\sqrt{2}$  factor from the expression given in ref.[8], because we use the standard normalization of the  $\lambda$  matrices,  $\text{tr}(\lambda^a \lambda^b) = \delta^{ab}/2$ .

where the gluons  $p_i$ , with  $i = 1, \dots, n$ , are all emitted with helicity  $\nu = +$ .

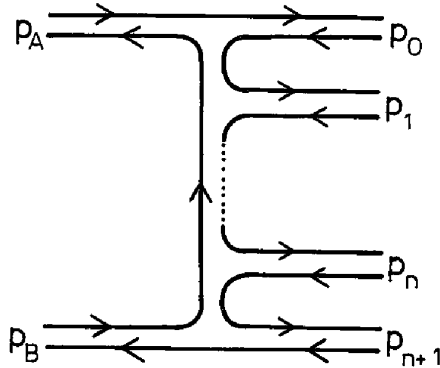


Figure 1: PT amplitude with color ordering  $[A, 0, \dots, n + 1, B]$ .

We put then eq.(13) back into eq.(6) and examine in detail all the color orderings, as we did in ref.[5], but here we do it at the amplitude level. We start with the ordering  $[A, 0, \dots, n + 1, B]$  (Fig.1). Using the spinor products (5) and the first of the identities (47) (Appendix B), the string of spinor products in the denominator of eq.(13) is

$$\langle p_A p_0 \rangle \cdots \langle p_{n+1} p_B \rangle \langle p_B p_A \rangle \simeq (-1)^{n+1} \langle p_A p_B \rangle^2 \prod_{i=0}^{n+1} p_{i\perp}. \quad (14)$$

It is easy to see by explicit calculation that every other color configuration, for which we keep fixed the position of gluons  $A$  and  $B$  in the color ordering and permute the outgoing gluons, gives a larger contribution to eq.(14) and so a subleading contribution, of  $\mathcal{O}(e^{-|y_i - y_j|})$ , to eq.(6). We note that untwisting the color lines on a configuration with permuted outgoing gluons, the color ordering we obtain is different from the rapidity ordering. Thus the leading color configuration in multiregge kinematics is the one whose untwisted lines respect the rapidity ordering (Fig.1).

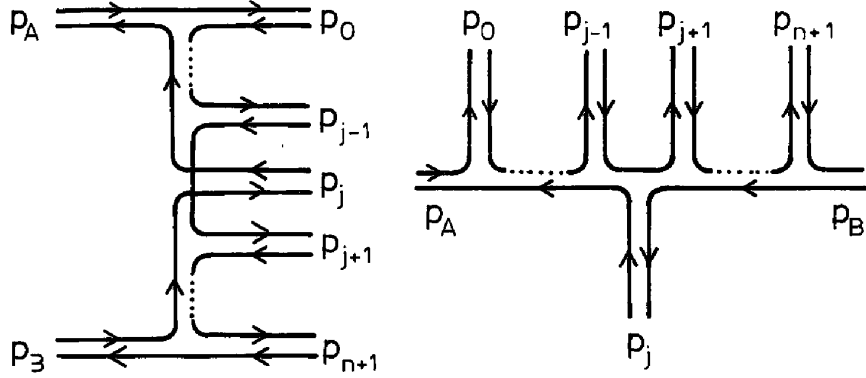


Figure 2: a) PT amplitude with color ordering  $[A, 0, \dots, j-1, j+1, \dots, n+1, B, j]$ , and b) its untwisted version on the two-sided plot.

Next, we move gluon  $B$  one step to the left and consider the color orderings  $[A, 0, \dots, j-1, j+1, \dots, n+1, B, j]$ , with  $j = 0, \dots, n+1$  (Fig.2a). Untwisting the color lines, we get gluon  $j$  on the back of the plot (Fig.2b). We compute then the string of spinor products,

$$\langle p_A p_0 \rangle \cdots \langle p_{j-1} p_{j+1} \rangle \cdots \langle p_{n+1} p_B \rangle \langle p_B p_j \rangle \langle p_j p_A \rangle \simeq (-1)^n \langle p_A p_B \rangle^2 \prod_{i=0}^{n+1} p_{i\perp}. \quad (15)$$

We note that the result is independent of which gluon we have taken to the back of the plot in Fig.2b. As compared to the string of spinor products in eq.(14) we have one more product with reversed order of the momenta; the first of the identities (47) (Appendix B) then entails one more minus sign in eq.(15). Next, we note that every permutation of the gluons on the front of the plot of Fig.2b gives a larger contribution to eq.(15) and so a subleading contribution, of  $\mathcal{O}(e^{-|y_i - y_j|})$ , to eq.(6). Thus the leading color configurations are the  $(n+2)$  configurations whose untwisted lines respect the rapidity ordering on the front of the plot of Fig.2b.

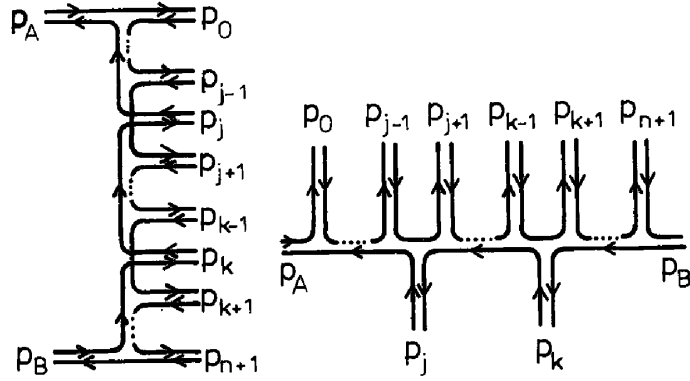


Figure 3: a) PT amplitude with color ordering  $[A, 0, \dots, j-1, j+1, \dots, k-1, k+1, \dots, n+1, B, k, j]$ , and b) its untwisted version on the two-sided plot.

Then we move gluon  $B$  further to the left and consider the color orderings  $[A, 0, \dots, j-1, j+1, \dots, k-1, k+1, \dots, n+1, B, k, j]$ , with  $j, k = 0, \dots, n+1$  and  $j < k$  (Fig.3a). Untwisting the color lines, we get gluons  $j$  and  $k$  on the back of the plot (Fig.3b). The related string of spinor products is,

$$\langle p_A p_0 \rangle \cdots \langle p_{j-1} p_{j+1} \rangle \cdots \langle p_{k-1} p_{k+1} \rangle \cdots \langle p_{n+1} p_B \rangle \langle p_B p_k \rangle \langle p_k p_j \rangle \langle p_j p_A \rangle \simeq (-1)^{n+1} \langle p_A p_B \rangle^2 \prod_{i=0}^{n+1} p_{i\perp}. \quad (16)$$

The same considerations we have done after eq.(15) apply to this configuration. We just note more that every permutation of the gluons on the front of the plot or on the back of the plot yields a larger contribution to eq.(16) and so a subleading contribution, of  $\mathcal{O}(e^{-|y_i - y_j|})$ , to eq.(6). Thus the leading color configurations are the  $\binom{n+2}{2}$  configurations whose untwisted lines respect the rapidity ordering on both the sides of the plot

of Fig.3b.

We can then proceed further by taking gluon  $B$  one more step to the left, i.e. by considering three gluons on the back of the plot, and so on. Taking gluon  $B$  all the way to the left, we will have exhausted all the  $(n+3)!$  noncyclic permutations of the color ordering  $[A, 0, \dots, B]$ . Substituting then eq.(13), (14), (15) and (16) into eq.(6), we obtain

$$\begin{aligned} iM(-p_A, -; p_0, +; \dots; p_{n+1}, +; -p_B, -) &\simeq i(-1)^{n+1} 2^{2+n/2} g^{n+2} \hat{s} \frac{1}{\prod_{i=0}^{n+1} p_{i\perp}} \\ &\times \text{tr} \left( \lambda^a \lambda^{d_0} \dots \lambda^{d_{n+1}} \lambda^b - \sum_{j=0}^{n+1} \lambda^a \lambda^{d_0} \dots \lambda^{d_{j-1}} \lambda^{d_{j+1}} \dots \lambda^{d_{n+1}} \lambda^b \lambda^{d_j} \right. \\ &\left. + \sum_{j < k} \lambda^a \lambda^{d_0} \dots \lambda^{d_{j-1}} \lambda^{d_{j+1}} \dots \lambda^{d_{k-1}} \lambda^{d_{k+1}} \dots \lambda^{d_{n+1}} \lambda^b \lambda^{d_k} \lambda^{d_j} + \dots \right), \end{aligned} \quad (17)$$

where the color orderings which contribute to eq.(17) in the multiregge kinematics are given by the  $2^{n+2}$  configurations which respect the rapidity ordering on the two-sided plot. Using nested commutators (cf. eq.(31)), eq.(17) may be written as,

$$\begin{aligned} iM(-p_A, -; p_0, +; \dots; p_{n+1}, +; -p_B, -) &\simeq \\ i(-1)^{n+1} 2^{2+n/2} g^{n+2} \hat{s} \frac{1}{\prod_{i=0}^{n+1} p_{i\perp}} \text{tr} &\left( \lambda^a \left[ \lambda^{d_0}, \left[ \lambda^{d_1}, \dots, \left[ \lambda^{d_{n+1}}, \lambda^b \right] \right] \right] \right). \end{aligned} \quad (18)$$

As noted after eq.(7), the configurations  $(+, +, -, \dots, -)$  are obtained by replacing the  $\langle pk \rangle$  products with  $[kp]$  products. Because of eq.(47) (Appendix B) this amounts to exchange  $\prod_i p_{i\perp}$  with  $\prod_i p_{i\perp}^*$  in eq.(18).

Finally, for the other helicity configurations of eq.(12) we obtain, from eq.(7) and the spinor products (5),

$$M(-p_A, +; p_0, -; \dots; p_{n+1}, +; -p_B, -) = M(-p_A, -; p_0, +; \dots; p_{n+1}, +; -p_B, -),$$

$$\begin{aligned}
M(-p_A, -; p_0, +; \dots; p_{n+1}, -; -p_B, +) &= M(-p_A, +; p_0, -; \dots; p_{n+1}, -; -p_B, +), \\
&= \left( \frac{p_{n+1\perp}}{p_{n+1\perp}^*} \right)^2 M(-p_A, -; p_0, +; \dots; p_{n+1}, +; -p_B, -),
\end{aligned} \tag{19}$$

where the gluons  $p_i$ , with  $i = 1, \dots, n$ , are as usual all emitted with helicity  $\nu = +$ .

## 4 The Fadin-Kureav-Lipatov amplitudes at fixed helicities

The tree-level amplitude for the production of  $n+2$  gluons in the multiregge kinematics has been computed in ref.[2] (Fig.4), and it is

$$\begin{aligned}
iM_{\nu_A \nu_0 \dots \nu_{n+1} \nu_B}^{ad_0 \dots d_{n+1} b} &\simeq 2i \hat{s} \left( ig f^{ad_0 c_1} \Gamma^{\mu_A \mu_0} \right) \epsilon_{\mu_A}^{\nu_A*}(p_A) \epsilon_{\mu_0}^{\nu_0}(p_0) \frac{1}{\hat{t}_1} \\
&\cdot \left( ig f^{c_1 d_1 c_2} C^{\mu_1}(q_1, q_2) \right) \epsilon_{\mu_1}^{\nu_1}(p_1) \frac{1}{\hat{t}_2} \\
&\cdot \dots \\
&\cdot \left( ig f^{c_n d_n c_{n+1}} C^{\mu_n}(q_n, q_{n+1}) \right) \epsilon_{\mu_n}^{\nu_n}(p_n) \frac{1}{\hat{t}_{n+1}} \\
&\cdot \left( ig f^{bd_{n+1} c_{n+1}} \Gamma^{\mu_b \mu_{n+1}} \right) \epsilon_{\mu_B}^{\nu_B*}(p_B) \epsilon_{\mu_{n+1}}^{\nu_{n+1}}(p_{n+1}),
\end{aligned} \tag{20}$$

where the  $\nu$ 's are the helicities, the  $q$ 's are the momenta of the gluons exchanged in the  $\hat{t}$  channel, and  $\hat{t}_i = q_i^2 \simeq -|q_{i\perp}|^2$ . The  $\Gamma$ -tensors are helicity-conserving tensors,

$$\begin{aligned}
\Gamma^{\mu_A \mu_0} &= g^{\mu_A \mu_0} - \frac{p_A^{\mu_0} p_B^{\mu_A} + p_B^{\mu_0} p_A^{\mu_A}}{p_A \cdot p_B} - \hat{t}_1 \frac{p_B^{\mu_0} p_B^{\mu_A}}{2(p_A \cdot p_B)^2}, \\
\Gamma^{\mu_B \mu_{n+1}} &= g^{\mu_B \mu_{n+1}} - \frac{p_A^{\mu_B} p_B^{\mu_{n+1}} + p_A^{\mu_{n+1}} p_B^{\mu_B}}{p_A \cdot p_B} - \hat{t}_{n+1} \frac{p_A^{\mu_{n+1}} p_A^{\mu_B}}{2(p_A \cdot p_B)^2},
\end{aligned} \tag{21}$$

and the Lipatov vertex [1] is

$$C^\mu(q_i, q_{i+1}) = \left[ (q_i + q_{i+1})_\perp^\mu - \left( \frac{\hat{s}_{Ai}}{\hat{s}} + 2 \frac{\hat{t}_{i+1}}{\hat{s}_{Bi}} \right) p_B^\mu + \left( \frac{\hat{s}_{Bi}}{\hat{s}} + 2 \frac{\hat{t}_i}{\hat{s}_{Ai}} \right) p_A^\mu \right], \quad (22)$$

with  $q_{i\perp}^\mu = (0, 0; q_{i\perp})$  and with the Mandelstam invariants as given in eq.(2). The  $\Gamma$ -tensors and the Lipatov vertex are gauge invariant.

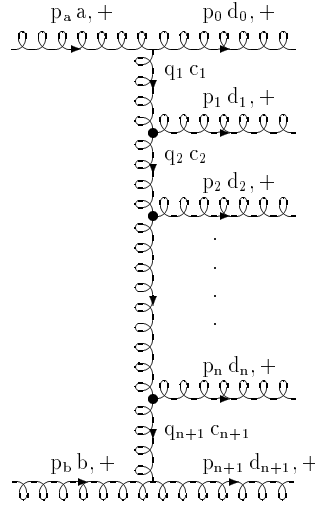


Figure 4: FKL amplitude for fixed gluon helicities. The blobs remind that Lipatov vertices are used for the gluon emissions along the ladder.

Helicity conservation at the production vertices for the first and the last gluon along the ladder in eq.(20) yields the four helicity configurations (12). For sake of comparison with the PT amplitudes we choose the helicity configuration of eq.(13). We invert then the momenta of gluons  $A$  and  $B$  and we obtain for the FKL amplitude the configuration of Fig.4. There is however no restriction in eq.(20) on the helicities of the gluons produced from the Lipatov vertices along the ladder.

We choose the representation (8) for the polarizations. As noted after eq.(11), this is equivalent to use a physical gauge. Then we must specify a reference vector with respect

to which we compute the polarization vectors in eq.(20), but thanks to gauge invariance the choice is arbitrary. For the polarization of gluons  $p_A$  and  $p_0$  we choose  $p_B$  as reference vector, while for the polarization of gluons  $p_B$  and  $p_i$  with  $i = 1, \dots, n+1$  we choose  $p_A$ . Following the nomenclature of ref.[10] we call the former a *right* gauge (R) and the latter a *left* gauge (L).

In order to facilitate the contraction with the Lipatov vertex in L or R gauges it is convenient to decompose a polarization vector in light-cone or Sudakov components. Using then the property (10) we obtain [10],

$$\begin{aligned}\epsilon_L^\mu(p) &= \epsilon_{L\perp}^\mu - \frac{p \cdot \epsilon_{L\perp}}{p \cdot p_A} p_A^\mu, \\ \epsilon_R^\mu(p) &= \epsilon_{R\perp}^\mu - \frac{p \cdot \epsilon_{R\perp}}{p \cdot p_B} p_B^\mu,\end{aligned}\tag{23}$$

with  $\epsilon_{L,R\perp}^\mu = (0, 0; \epsilon_{L,R\perp})$ , and  $\epsilon_{L,R}^2 = \epsilon_{L,R\perp}^2 = -1$ .

Contracting the polarization vector in the L gauge (23) with the Lipatov vertex (22), we have [10], [11]

$$\epsilon_L(p_i) \cdot C(q_i, q_{i+1}) = 2 |q_{i+1\perp}|^2 \left( \frac{q_{i+1\perp}^\mu}{|q_{i+1\perp}|^2} + \frac{p_{i\perp}^\mu}{|p_{i\perp}|^2} \right) \epsilon_{L\perp}^\mu.\tag{24}$$

Using eq.(53) (Appendix C) and the complex notation (36) (Appendix A) we may write the contraction (24) for the helicity  $\nu = +$  as

$$\epsilon_L^+(p_i) \cdot C(q_i, q_{i+1}) = -\sqrt{2} \frac{q_{i\perp}^* q_{i+1\perp}}{p_{i\perp}^*},\tag{25}$$

from which, using the conversion table (55) (Appendix C) between the representations (8) and (23), the contraction of the Lipatov vertex with the gluon polarization in eq.(20) is,

$$\epsilon^+(p_i, p_A) \cdot C(q_i, q_{i+1}) = \sqrt{2} \frac{q_{i\perp}^* q_{i+1\perp}}{p_{i\perp}}.\tag{26}$$

From eq.(49) (Appendix C), the contractions of the helicity-conserving tensors (21) with the gluon polarizations are<sup>2</sup>,

$$\begin{aligned}\Gamma^{\mu_B \mu_{n+1}} \epsilon_{\mu_B}^{+*}(p_B, p_A) \epsilon_{\mu_{n+1}}^+(p_{n+1}, p_A) &= -\frac{p_{n+1\perp}^*}{p_{n+1\perp}}, \\ \Gamma^{\mu_A \mu_0} \epsilon_{\mu_A}^{+*}(p_A, p_B) \epsilon_{\mu_0}^+(p_0, p_B) &= -1.\end{aligned}\quad (27)$$

Substituting eq.(26) and (27) into eq.(20), the FKL amplitude in the helicity configuration of eq.(13) becomes

$$\begin{aligned}iM(p_A, +; p_0, +; \dots; p_{n+1}, +; p_B, +) &= \\ 2i(-1)^n 2^{n/2} (ig)^{n+2} \hat{s} \frac{1}{\prod_{i=0}^{n+1} p_{i\perp}} f^{ad_0 c_1} f^{c_1 d_1 c_2} \dots f^{c_n d_n c_{n+1}} f^{b d_{n+1} c_{n+1}} &.\end{aligned}\quad (28)$$

Next, we need to convert the product of structure constants into the trace of a product of  $\lambda$ -matrices. From the algebra of the  $\lambda$ -matrices we have

$$\begin{aligned}f^{abc} &= -2i \text{tr}([\lambda^a, \lambda^b] \lambda^c), \\ \sum_a \lambda_{ij}^a \lambda_{kl}^a &= \frac{1}{2} \left[ \delta_{il} \delta_{jk} - \frac{1}{N_c} \delta_{ij} \delta_{kl} \right],\end{aligned}\quad (29)$$

from which, using the antisymmetry of the structure constants and the cyclicity of the trace, we have

$$f^{abz} \text{tr}(\lambda^z, [\lambda^c, [\lambda^d, \dots, [\lambda^x, \lambda^y]]]) = -i \text{tr}(\lambda^a [\lambda^b, [\lambda^c, [\lambda^d, \dots, [\lambda^x, \lambda^y]]]]). \quad (30)$$

Using eq.(29) and (30), it is then easy to see that,

$$f^{ad_0 c_1} f^{c_1 d_1 c_2} \dots f^{c_n d_n c_{n+1}} f^{b d_{n+1} c_{n+1}} =$$

---

<sup>2</sup>Note that we obtain the result of eq.(27) also by using the simpler helicity-conserving tensor  $g^{\mu\nu}$ , however  $g^{\mu\nu}$  is not gauge invariant as it can be seen by using it and changing reference vectors in eq.(27).

$$\begin{aligned}
& -2(-i)^{n+2} \text{tr} \left( \lambda^a \left[ \lambda^{d_0}, \left[ \lambda^{d_1}, \dots, \left[ \lambda^{d_{n+1}}, \lambda^b \right] \right] \right] \right) = \\
& -2(-i)^{n+2} \text{tr} \left( \lambda^a \lambda^{d_0} \dots \lambda^{d_{n+1}} \lambda^b - \sum_{j=0}^{n+1} \lambda^a \lambda^{d_0} \dots \lambda^{d_{j-1}} \lambda^{d_{j+1}} \dots \lambda^{d_{n+1}} \lambda^b \lambda^{d_j} \right. \\
& \left. + \sum_{j < k} \lambda^a \lambda^{d_0} \dots \lambda^{d_{j-1}} \lambda^{d_{j+1}} \dots \lambda^{d_{k-1}} \lambda^{d_{k+1}} \dots \lambda^{d_{n+1}} \lambda^b \lambda^{d_k} \lambda^{d_j} + \dots \right) ,
\end{aligned} \tag{31}$$

which shows that also for the FKL amplitudes the only configurations which contribute are the  $2^{n+2}$  color configurations which respect the rapidity ordering on the two-sided plot of Fig.2 and 3.

Replacing eq.(31) into eq.(28), we find it in agreement with eq.(18), thereby proving that the PT amplitudes and the FKL amplitudes coincide in the high-energy limit.

The configuration with all the helicities  $\nu = -$  is obtained by replacing the complex conjugates of eq.(26) and (27) into eq.(20), which amounts to change  $\prod_i p_{i\perp}$  with  $\prod_i p_{i\perp}^*$  in eq.(28), in agreement with what we noted after eq.(18).

Also the calculation of the FKL amplitude for the other helicity configurations of eq.(12) is obtained from the one of eq.(28), by taking the suitable complex conjugates of the contractions (27),

$$\begin{aligned}
M(p_A, -; p_0, -; \dots; p_{n+1}, +; p_B, +) &= M(p_A, +; p_0, +; \dots; p_{n+1}, +; p_B, +) , \\
M(p_A, +; p_0, +; \dots; p_{n+1}, -; p_B, -) &= M(p_A, -; p_0, -; \dots; p_{n+1}, -; p_B, -) , \\
&= \left( \frac{p_{n+1\perp}}{p_{n+1\perp}^*} \right)^2 M(p_A, +; p_0, +; \dots; p_{n+1}, +; p_B, +) ,
\end{aligned} \tag{32}$$

with helicities  $\nu_i = +$  and  $i = 1, \dots, n$ . Eq.(32) is in agreement with eq.(19).

Finally, we note that the two helicities of each gluon produced along the ladder exchanged in the  $\hat{t}$  channel contribute on equal footing to the FKL amplitude (20).

Indeed changing the helicity of gluon  $p_i$  we must take the complex conjugate of eq.(26), and we obtain that the amplitude (28) changes only by a phase,

$$M(p_A, +; p_0, +; \dots; p_{j-1}, +; p_j, -; p_{j+1}, +; \dots; p_{n+1}, +; p_B, +) = \frac{p_{i\perp} q_{i\perp} q_{i+1\perp}^*}{p_{i\perp}^* q_{i\perp}^* q_{i+1\perp}} M(p_A, +; p_0, +; \dots; p_{n+1}, +; p_B, +). \quad (33)$$

## 5 Conclusions

In this work we have given a unified description of tree-level multigluon amplitudes in the multiregge kinematics. Representing the color flows in terms of color lines in the fundamental representation of  $SU(N_c)$ , we have shown that the leading color configurations for the PT amplitudes and for the FKL amplitudes are the ones whose untwisted color lines are ordered in rapidity on a two-sided plot. For the helicity configurations they have in common, we have shown that the PT amplitudes and the FKL amplitudes are equal, without any phase arbitrariness.

A corollary of the calculation of the FKL amplitude at fixed helicity is that changing the helicity of a gluon along the gluon ladder changes the FKL amplitude only by a phase, thus the two helicities of each gluon emitted along the ladder contribute equally to an unpolarized production rate computed from the FKL amplitude.

Finally, as remarked in the Introduction, including the leading logarithmic contributions, in  $\ln(\hat{s}/\hat{t})$ , of the loop corrections to eq.(20) modifies the propagator of the gluon of momentum  $q_i$  exchanged in the  $\hat{t}$  channel by the factor [2]

$$\frac{1}{\hat{t}_i} \rightarrow \frac{1}{\hat{t}_i} \left( -\frac{\hat{s}_{i-1,i}}{\hat{t}_i} \right)^{\alpha(\hat{t}_i)}, \quad (34)$$

with  $i = 1, \dots, n$  and  $\alpha(\hat{t}_i)$  a function of the loop-momentum integral. Thus the FKL amplitude with the leading-logarithmic loop corrections retains the ladder structure of eq.(20) and the color structure of eq.(31), so the dominant color configurations are still the ones whose untwisted lines are ordered in rapidity on the two-sided plot. Even though this is a simple observation from the standpoint of the FKL amplitudes, it is far from being obvious when we consider the color decomposition of multigluon amplitudes in a helicity basis, since the color structure of the tree-level amplitudes (6) does not describe all the possible color configurations of  $n$  gluons, more configurations appearing in the color decomposition at the loop level [12].

Thus the invariance of the color structure of the FKL amplitude from the tree level to the loop level seems to imply that the additional color configurations that appear in the decomposition of loop-level multigluon amplitudes in a helicity basis should not give a leading contribution in the multiregge kinematics.

## Acknowledgements

I wish to thank Lev Lipatov and Mark Wüsthoff for useful discussions.

## A Multiparton kinematics

We consider the production of  $n + 2$  gluons of momentum  $p_i$ , with  $i = 0, \dots, n + 1$  and  $n \geq 0$ , in the scattering between two gluons of momenta  $p_A$  and  $p_B$ . Naming the momentum in the beam direction,  $p_{||}$ , and in plane transverse to the beam,  $p_{\perp}$ , and using

light-cone coordinates,  $p^\pm = p_0 \pm p_{||}$ , with scalar product  $p \cdot q = (p^+ q^- + p^- q^+)/2 - p_\perp \cdot q_\perp$ , the gluon 4-momenta are,

$$\begin{aligned} p_A &= (p_A^+, 0; 0, 0) , \\ p_B &= (0, p_B^-; 0, 0) , \\ p_i &= (|p_{i\perp}|e^{y_i}, |p_{i\perp}|e^{-y_i}; |p_{i\perp}| \cos \phi_i, |p_{i\perp}| \sin \phi_i) , \end{aligned} \quad (35)$$

where to the left of the semicolon we have the + and - components, and to the right the transverse components.  $y$  is the gluon rapidity and  $\phi$  is the azimuthal angle between the vector  $p_\perp$  and an arbitrary vector in the transverse plane. Throughout the paper we use the complex notation for the transverse momenta,

$$p_\perp = |p_\perp|e^{i\phi}. \quad (36)$$

From the momentum conservation,

$$\begin{aligned} 0 &= \sum_{i=0}^{n+1} p_{i\perp} , \\ p_A^+ &= \sum_{i=0}^{n+1} |p_{i\perp}|e^{y_i} , \\ p_B^- &= \sum_{i=0}^{n+1} |p_{i\perp}|e^{-y_i} , \end{aligned} \quad (37)$$

the Mandelstam invariants may be written as,

$$\begin{aligned} \hat{s} &= 2p_A \cdot p_B = \sum_{i,j=0}^{n+1} |p_{i\perp}| |p_{j\perp}| e^{y_i - y_j} \\ \hat{s}_{Ai} &= -2p_A \cdot p_i = -\sum_{j=0}^{n+1} |p_{i\perp}| |p_{j\perp}| e^{-(y_i - y_j)} \\ \hat{s}_{Bi} &= -2p_B \cdot p_i = -\sum_{j=0}^{n+1} |p_{i\perp}| |p_{j\perp}| e^{y_i - y_j} \\ \hat{s}_{ij} &= 2p_i \cdot p_j = 2|p_{i\perp}| |p_{j\perp}| [\cosh(y_i - y_j) - \cos(\phi_i - \phi_j)] . \end{aligned} \quad (38)$$

## B Massless-spinor algebra

The spinors (4) are normalized as<sup>3</sup>

$$\langle p \pm | \gamma_\mu | p \pm \rangle = 2p_\mu, \quad (39)$$

and their relative phases are chosen so that under the charge-conjugation operation  $C$

$$|p \mp\rangle = |p \pm\rangle^c = C|p \pm\rangle^*, \quad (40)$$

with charge-conjugation matrix satisfying the algebra [13]

$$\gamma_\mu = -C\gamma_\mu^*C^{-1}, \quad (41)$$

$$C = C^{-1} = C^\dagger = C^T. \quad (42)$$

Eq.(41) determines  $C$  up to a phase  $C = e^{i\alpha}\gamma_2$ , and the further condition (42) fixes it as  $C = \pm i\gamma_2$ . From eq.(41) the transposed spinor transforms as,

$$\langle p \mp | = {}^c\langle p \pm | = -{}^*\langle p \pm | C. \quad (43)$$

We use the chiral representation of the  $\gamma$ -matrices [13],

$$\gamma^0 = \begin{pmatrix} 0 & I \\ I & 0 \end{pmatrix}, \quad \gamma^i = \begin{pmatrix} 0 & -\sigma^i \\ \sigma^i & 0 \end{pmatrix}, \quad (44)$$

with  $I$  the  $2 \times 2$  unit matrix and  $\sigma^i$  the Pauli matrices. Solving then the Dirac equation  $\not{p}\psi(p) = 0$  and using the normalization condition (39) and the complex notation (36),

---

<sup>3</sup>See ref.[8] for a summary of the properties of the spinor algebra.

the spinors for the gluon momenta (35) are,

$$\begin{aligned}
\psi_+(p) &= e^{i\gamma} \begin{pmatrix} \sqrt{p^+} \\ \sqrt{p^-} e^{i\phi} \\ 0 \\ 0 \end{pmatrix} & \psi_-(p) &= e^{-i\gamma} \begin{pmatrix} 0 \\ 0 \\ \sqrt{p^-} e^{-i\phi} \\ -\sqrt{p^+} \end{pmatrix} \\
\psi_+(p_A) &= e^{i\alpha} \begin{pmatrix} \sqrt{p_A^+} \\ 0 \\ 0 \\ 0 \end{pmatrix} & \psi_-(p_A) &= e^{-i\alpha} \begin{pmatrix} 0 \\ 0 \\ 0 \\ -\sqrt{p_A^+} \end{pmatrix} \\
\psi_+(p_B) &= e^{i\beta} \begin{pmatrix} 0 \\ \sqrt{p_B^-} \\ 0 \\ 0 \end{pmatrix} & \psi_-(p_B) &= e^{-i\beta} \begin{pmatrix} 0 \\ 0 \\ \sqrt{p_B^-} \\ 0 \end{pmatrix}
\end{aligned} \tag{45}$$

where the relative sign between  $\psi_+(p)$  and  $\psi_-(p)$  is fixed by choosing the charge-conjugation matrix as  $C = i\gamma_2$ . The overall phases  $e^{i\gamma}$ ,  $e^{i\alpha}$  and  $e^{i\beta}$  are of course arbitrary. Without losing generality we fix them to 1. Using the spinor representation (45), the spinor products for the momenta (35) are

$$\begin{aligned}
\langle p_i p_j \rangle &= \frac{p_j^+ p_{i\perp} - p_i^+ p_{j\perp}}{\sqrt{p_i^+ p_j^+}}, \\
\langle p_A p_i \rangle &= -\sqrt{\frac{p_A^+}{p_i^+}} p_{i\perp}, \\
\langle p_i p_B \rangle &= -\sqrt{\frac{p_B^-}{p_i^-}} |p_{i\perp}|, \\
\langle p_A p_B \rangle &= -\sqrt{\hat{s}}.
\end{aligned} \tag{46}$$

Using the spinors (45), the momentum conservation (37) and the Mandelstam invariants (38), it is straightforward to check that the spinor products (46) satisfy the identities,

$$\begin{aligned}\langle pk \rangle &= -\langle kp \rangle, \\ \langle pk \rangle^* &= [kp], \\ \langle pk \rangle [kp] &= 2p \cdot k = |\hat{s}_{pk}|,\end{aligned}\tag{47}$$

which entail that the spinor products may be regarded as the complex square roots of the Mandelstam invariants.

## C The gluon polarizations

For the gluon polarizations we use the representation (8)

$$\epsilon_\mu^\pm(p, k) = \pm \frac{\langle p \pm | \gamma_\mu | k \pm \rangle}{\sqrt{2} \langle k \mp | p \pm \rangle}.\tag{48}$$

Using the representations (44) for the  $\gamma$ -matrices and (45) for the spinors, we obtain

$$\begin{aligned}\epsilon_\mu^+(p_i, p_A) &= -\frac{p_{i\perp}^*}{p_{i\perp}} \left( \frac{\sqrt{2} p_{i\perp}}{p_i^-}, 0; \frac{1}{\sqrt{2}}, \frac{i}{\sqrt{2}} \right), \\ \epsilon_\mu^+(p_B, p_A) &= -\left( 0, 0; \frac{1}{\sqrt{2}}, \frac{i}{\sqrt{2}} \right), \\ \epsilon_\mu^+(p_A, p_B) &= \left( 0, 0; \frac{1}{\sqrt{2}}, -\frac{i}{\sqrt{2}} \right), \\ \epsilon_\mu^+(p_i, p_B) &= \left( 0, \frac{\sqrt{2} p_{i\perp}^*}{p_i^+}; \frac{1}{\sqrt{2}}, -\frac{i}{\sqrt{2}} \right),\end{aligned}\tag{49}$$

in light-cone coordinates.

The decomposition of a polarization vector in light-cone or Sudakov components is [10],

$$\begin{aligned}\epsilon_L^\mu(p) &= \epsilon_{L\perp}^\mu - \frac{p \cdot \epsilon_{L\perp}}{p \cdot p_A} p_A^\mu, \\ \epsilon_R^\mu(p) &= \epsilon_{R\perp}^\mu - \frac{p \cdot \epsilon_{R\perp}}{p \cdot p_B} p_B^\mu.\end{aligned}\quad (50)$$

The polarizations  $\epsilon_L^\mu(p)$ ,  $\epsilon_R^\mu(p)$  and  $\epsilon_{L\perp}^\mu$ ,  $\epsilon_{R\perp}^\mu$  for a momentum  $p$  not in the beam direction are related by a gauge transformation,

$$\epsilon_R^\mu(p) = \epsilon_L^\mu(p) + 2 \frac{\epsilon_{L\perp} \cdot p}{|p_\perp|^2} p^\mu. \quad (51)$$

Using the complex notation (36) the gauge transformation (51) for the transverse components may be written as,

$$\epsilon_{R\perp}(p) = -\frac{p_\perp}{p_\perp^*} \epsilon_{L\perp}^*(p), \quad (52)$$

for  $p \neq p_A$  or  $p_B$ . We impose then the following standard polarizations,

$$\epsilon_{L\perp}^{\mu\pm}(p) = \left(0, 0; \frac{1}{\sqrt{2}}, \pm \frac{i}{\sqrt{2}}\right), \quad (53)$$

$$\epsilon_{L\perp}^{\mu\pm}(p_B) = \epsilon_{R\perp}^{\mu\mp}(p_A) = \left(0, 0; \frac{1}{\sqrt{2}}, \pm \frac{i}{\sqrt{2}}\right). \quad (54)$$

We determine  $\epsilon_L^\mu(p)$  using eq.(53) in the definition (50), then we find  $\epsilon_R^\mu(p)$  using the gauge transformations (51) and (52) on  $\epsilon_L^\mu(p)$ . Finally,  $\epsilon_L^\mu(p_B)$  and  $\epsilon_R^\mu(p_A)$  are given by eq.(54) and the definitions (50). Comparing the results with eq.(49), we obtain the following conversion table among the representations (48) and (50) of the polarizations

$$\begin{aligned}\epsilon_\mu^+(p_i, p_A) &= -\frac{p_{i\perp}^*}{p_{i\perp}} \epsilon_{L\mu}^+(p_i), \\ \epsilon_\mu^+(p_i, p_B) &= -\frac{p_{i\perp}^*}{p_{i\perp}} \epsilon_{R\mu}^+(p_i)\end{aligned}\quad (55)$$

$$\begin{aligned}\epsilon_\mu^+(p_B, p_A) &= -\epsilon_{L\mu}^+(p_B), \\ \epsilon_\mu^+(p_A, p_B) &= \epsilon_{R\mu}^+(p_A).\end{aligned}$$

## References

- [1] L.N. Lipatov, *Yad. Fiz.* **23**, 642 (1976) [*Sov. J. Nucl. Phys.* **23**, 338 (1976)].
- [2] E.A. Kuraev, L.N. Lipatov and V.S. Fadin, *Zh. Eksp. Teor. Fiz.* **71**, 840 (1976) [*Sov. Phys. JETP* **44**, 443 (1976)].
- [3] E.A. Kuraev, L.N. Lipatov and V.S. Fadin, *Zh. Eksp. Teor. Fiz.* **72**, 377 (1977) [*Sov. Phys. JETP* **45**, 199 (1977)];  
Ya.Ya. Balitsky and L.N. Lipatov, *Yad. Fiz.* **28** 1597 (1978) [*Sov. J. Nucl. Phys.* **28**, 822 (1978)].
- [4] S.J. Parke and T. Taylor, *Phys. Rev. Lett.* **56**, 2459 (1986).
- [5] V. Del Duca, *Phys. Rev. D* **48**, 5133 (1993).
- [6] G. Veneziano, *Phys. Lett.* **43B**, 413 (1973);  
J.D. Bjorken, *Phys. Rev. D* **45**, 4077 (1992).
- [7] Z. Xu, D.-H. Zhang and L. Chang, *Nucl. Phys.* **B291**, 392 (1987).
- [8] M.L. Mangano and S.J. Parke, *Phys. Rep.* **200**, 301 (1991).
- [9] D.A. Kosower, *Nucl. Phys.* **B335**, 23 (1990).
- [10] L.N. Lipatov, *Nucl. Phys.* **B365**, 614 (1991).

- [11] J. Bartels and M. Wüsthoff, preprint DESY 94-016.
- [12] Z. Bern and D.A. Kosower, Nucl. Phys. **B362**, 389 (1991).
- [13] J.D. Bjorken and S.D. Drell, *Relativistic Quantum Mechanics*, McGraw-Hill, 1964.